Glycoconj J (2013) 30:523–536
DOI 10.1007/s10719-012-9452-8

Characterization of *N*- and *O*-linked glycosylation changes in milk of the tammar wallaby (*Macropus eugenii*) over lactation

Katherine Wongtrakul-Kish · Daniel Kolarich · Dana Pascovici · Janice L. Joss · Elizabeth Deane · Nicolle H. Packer

Received: 8 July 2012 / Revised: 6 September 2012 / Accepted: 11 September 2012 / Published online: 10 October 2012

Abstract As one of several biologically active compounds in milk, glycoproteins have been indicated to be involved in the protection of newborns from bacterial infection. As much of the physical and immune development of the tammar wallaby (*Macropus eugenii*) young occurs during the early phases of lactation and not *in utero*, the tammar is a model species for the characterization of potential developmental support agents provided by maternal milk.

In the present study, the *N*- and *O*-linked glycans from tammar wallaby milk glycoproteins from six individuals at different lactation time points were subjected to glycomics analyses using porous graphitized carbon liquid chromatography electrospray ionization mass spectrometry. Structural characterization identified a diverse range of glycan structures on wallaby milk glycoproteins including sialylated, sulphated, core fucosylated and *O*-fucosylated structures. 30 % of *N*-linked structures contained a core (α1-6) fucose. Several of these structures may play roles in development, and exhibit statistically significant temporal changes over the lactation period. The *N*-glycome was found to contain structures with NeuGc residues, while in contrast the *O*-glycome did not. *O*-fucosylated structures were identified in the early stages of lactation indicating a potential role in the early stages of development of the pouch young. Overall the results suggest that wallaby milk contains structures known to have developmental and immunological significance in human milk and reproduction in other animals, highlighting the importance of glycoproteins in milk.

Keywords Glycoproteins · Lactation · Wallaby · Milk · Glycosylation

Electronic supplementary material The online version of this article (doi:10.1007/s10719-012-9452-8) contains supplementary material, which is available to authorized users.

K. Wongtrakul-Kish · D. Kolarich · N. H. Packer (✉)
Biomolecular Frontiers Research Centre, Department of Chemistry and Biomolecular Sciences, Macquarie University,
Building E8C Room 307,
North Ryde, NSW 2109, Australia
e-mail: nicki.packer@mq.edu.au

J. L. Joss · E. Deane
Department of Biological Sciences, Macquarie University,
North Ryde, NSW 2109, Australia

D. Pascovici
Australian Proteome Analysis Facility, Macquarie University,
North Ryde, NSW 2109, Australia

Present Address:
D. Kolarich
Department of Biomolecular Systems,
Max Planck Institute of Colloids and Interfaces,
14424 Potsdam, Germany

Present Address:
J. L. Joss
Centre for Vascular Research, Lowy Cancer Research Centre,
University of New South Wales,
Randwick, Australia

Present Address:
E. Deane
The Chancellery, Australian National University,
Canberra 0200, ACT, Australia

Abbreviations

PGC	Porous Graphitized Carbon
LC	Liquid Chromatography
ESI-MS	Electrospray Ionisation Mass Spectrometry
PNGase F	N-Glycosidase F
BPC	Base Peak Chromatogram
EIC	Extracted Ion Chromatogram
Hex	Hexose
HexNAc	*N*-acetylhexosamine
NeuAc	*N*-acetylneuraminic acid
NeuGc	*N*-glycolylneuraminic acid
Man	Mannose
GlcNAc	*N*-acetylglucosamine

Sulph	Sulphate
IgY	Immunoglobulin Y
IgG	Immunoglobulin G

Introduction

In all mammalian groups studied to date, a delay in the development of the immune system has been observed [1]. While any delay would appear to be disadvantageous to newborns in combating infection, they can however receive immune system protective agents from their mothers *via* the placenta whilst *in utero* and then *via* their mother's milk after birth [1]. In humans, due to breast milk's unique blend of compounds, breast fed infants have been shown to be less affected by gastric infections [2]. Studies investigating the gut flora of breast-fed babies in comparison to formula-fed babies have demonstrated differences in bacterial strain colonization [3, 4]. Also, the survival rate of breast fed infants is significantly higher compared to formula fed babies [5].

The marsupial tammar wallaby (*Macropus eugenii*) has been shown to be a model species for investigation of changes in mammalian milk composition in relation with early infant development. The pouch young's underdeveloped state at birth results in complete reliance on their mother's milk for nutritional and developmental support in the first 100 days of lactation before they leave the mother's pouch and begin to consume food from their surroundings during the next 200 days of lactation [6]. Tammar milk composition changes over the 300 day lactation period in accordance with the developmental needs of the pouch young [7]. For example, major whey proteins in wallaby milk that are known to be involved in immune protection change throughout lactation depending on the development of the young's immune system [6]. Although it is not certain exactly when each pouch young immune development phase begins and ends, the lactation period can be approximately broken up according to the three phases: incompetent (first ~35 days), transitional (~45 to 105 days) and competent (~115 days onwards) [6]. Because most of the physical and immune development of the pouch young occurs *ex-utero* after a relatively short 26 day gestation period [8], relationships between milk composition and pouch young development needs can be proposed.

Glycans make up a large percentage of innate immune system components and can be found either as free oligosaccharides or as glycoconjugates such as glycoproteins, glycosaminoglycans, glycolipids or mucins [9]. Glycans are involved in a number of different functions and cellular processes, such as cell adhesion and signaling [10–12]. This involvement mediates different downstream processes, one of which is immune system development and protection. In human milk, it is hypothesized that a mechanism of immune protection is provided by the ability of free glycans to bind to foreign bacteria and thus carry them out of the body through the digestive process [9]. Infection is therefore avoided as bacteria are prevented from binding to intestinal glycan receptors in the gut epithelium. This hypothesis is supported as many of these glycans remain intact during their passage through the alimentary canal and digestive system [13]. Thus it can be assumed that a proportion of the glycan constituents of glycoproteins remain unaffected by the digestive process and present a set of binding glycan epitopes in addition to the free sugars. Milk glycans have also been shown to influence the development of the gut microbiome by their role as a growth substrate. Marcobal *et al.* [14] showed that *Bifidobacterium longum* subsp. *infantis*, *Bacteroides fragilis*, and *Bacteroides vulgatus* strains metabolized human milk oligosaccharides with high efficiency, whereas *Enterococcus*, *Streptococcus*, *Veillonella*, *Eubacterium*, *Clostridium*, and *Escherichia coli* strains had reduced growth or did not grow at all when fed with a mixture of milk oligosaccharides. Thus the milk glycome (and glycoproteome) can act both by providing decoy binding sites for pathogens and as prebiotics for enrichment of beneficial bacteria.

The free oligosaccharides of tammar wallaby milk have previously been investigated, revealing the presence of neutral oligo- and polysaccharides, and sialylated saccharides [15–20]. The presence of free sugars in tammar milk appears to be tightly controlled according to the needs of the pouch young. Messer and Green [17] observed in two wallaby mothers, that milk rich with oligosaccharides was produced for newborn young while concurrently producing milk comprising mainly monosaccharides in a separate teat for young no longer permanently residing in the pouch. At parturition, only lactose is present in tammar milk, followed by the presence of larger oligosaccharides and hexose, increasing in concentrations from day 4 onwards of lactation before declining rapidly at around 170 days [17]. By around 224 days, monosaccharides make up the majority of tammar milk content, including galactose, glucose, glucosamine, galactosamine and sialic acid moieties [17].

In the present study, the protein bound glycome of tammar wallaby milk was explored in relation to the development of pouch young using the well established system of porous graphitized carbon (PGC) liquid chromatography (LC) electrospray ionization mass spectrometry (ESI-MS) [21–23]. The protein bound oligosaccharides were monitored at different stages of the lactation period reflecting the different immune system development stages of the wallaby young. Although the tammar milk free oligosaccharides have been characterized [20], no previous analysis has been conducted on glycoproteins in tammar wallaby milk and the changes in glycosylation over lactation time.

Results

The *N*-glycome of wallaby milk glycoproteins

Glycoproteins were isolated from 2 μL of wallaby milk from different stages of lactation using precipitation with chloroform and methanol. After immobilisation of the re-solubilised proteins on PVDF membrane, *N*-glycans were released by PNGase F, isolated, and the global profile of the *N*-linked oligosaccharides (*N*-glycome) characterised by PGC-LC ESI-MS/MS (Fig. 1a). Inter-animal variability appeared to be minimal as seen from the average *N*-glycan MS profiles of six different individuals at similar lactation time points (Figure 1, Supp data). However, comparison of the *N*-glycan PGC-LC Base Peak Chromatograms (BPC), that more accurately defines the isomeric heterogeneity of the glycans, at different lactation times, indicated that global glycosylation changes occurred over the lactation period in all individuals (Figure 2, Supp data).

PGC-LC ESI-MS/MS for differentiation of N-glycan isomeric structures

Many glycan masses are the sum of compositional isomers with different branched structures. Investigation and differentiation of these isomeric structures by MS/MS was facilitated by the use of online PGC-LC before ESI-MS/MS detection as exemplified by the example shown in Fig. 2. A doubly charged signal with the *m/z* of $[M\text{-}2H]^{2-}$ = 965.9 Da was found to elute as five chromatographic peaks. This mass can correspond to two different monosaccharide compositions: $HexNAc_4Hex_5NeuAc$ (N10, Table 1) or $HexNAc_4Hex_4FucNeuGc$ (N11, Table 1). While three of the peaks could be assigned by MS/MS fragmentation to the composition $HexNAc_4Hex_5NeuAc$, with each structure differing only in the position and linkage of NeuAc, the peak eluting at approximately 53 min in Fig. 2c was clearly assigned as a (α1,6) core fucosylated biantennary structure (Fig. 2c) with one NeuGc on the 3′ arm antenna. Digestion with (α-2,3–6) neuraminidase and (ß-1,4) galactosidase confirmed the PGC-LC ESI-MS/MS results (Fig. 2c & d). The four *N*-acetylneuraminic acid containing *m/z* $[965.9]^{2-}$ isomers were differentiated using the *m/z* 979.3 diagnostic fragment 'D' ion for 6′ arm linked *N*-acetylneuraminic acid residues and matched to the elution profile of the same structures from Nakano *et al.* [24]. D-ions are produced from cleavages around the branching mannose residue of the *N*-glycan chitobiose core, causing the loss of the core and the 3′ arm, therefore providing 6′arm-specific compositional information [25].

Statistical analysis of the temporal changes of the N-glycome

Overall, 37 structures were identified by MS/MS and/or retention time over all samples (see Table 1). 62 % of identified *N*-glycan structures were of the biantennary type and 30 % of structures contained a core (α1,6) fucose. *N*-glycans containing both NeuAc and NeuGc were found on wallaby milk glycoproteins with 17 structures containing NeuAc (46 %) being more prominent compared to NeuGc (16 %), and one structure containing both NeuAc and NeuGc (n11, Table 1).

Statistical analysis using a linear mixed-effects model of the most abundant 16*N*-glycan masses (see N1-N16, Table 1) uncovered eight structures exhibiting temporal changes consistently across individuals between at least two time points ($p<0.05$, Table 1). These changes were displayed through box plots in order to graph the $\log_e$ normalized percentage abundances of each structure from all six individuals over time (Fig. 3). Five of these eight structures were core fucosylated (N1, N2, N11, N4 and N6) with three of these five (N1, N4 and N6) exhibiting the same temporal trend starting with an initial relatively low abundance at the incompetent immune development stage with

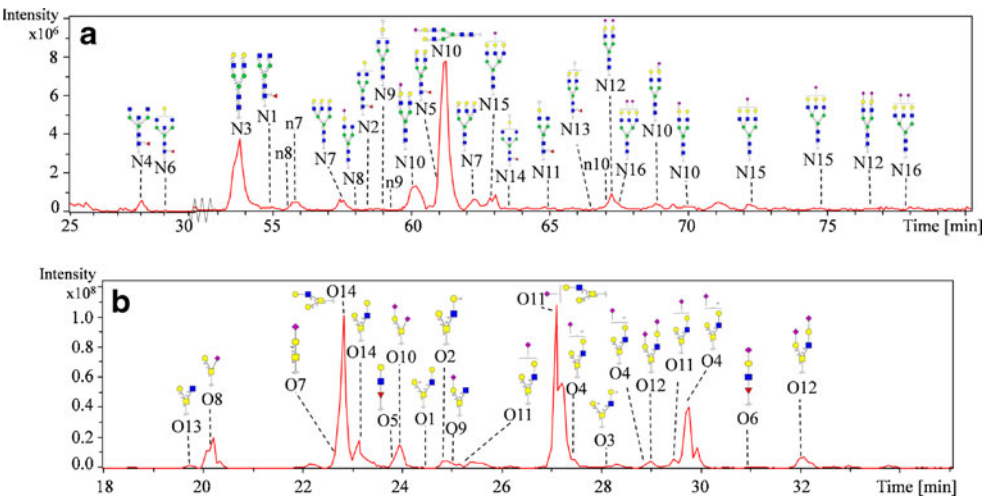

Fig. 1 Base peak chromatograms of a representative tammar wallaby milk *N*-glycan (**a**) and *O*-glycan sample (**b**). N/n=*N*-linked oligosaccharide, O=*O*-linked oligosaccharide. Details of these structures are shown in Tables 1 and 2

a subsequent increase over the transitional stage, followed by subsequent decrease in the final competent stage (Fig. 3a). The remaining two core fucosylated structures (N2 and N11) showed a significant increase in abundance over the lactation period (Fig. 3b).

Two trianntenary *N*-glycans, N7 and N15 (Table 1), showed an initial relatively high abundance at the incompetent immune stage, dropping during the transitional stage and followed by an increase in abundance at the final competent stage (Fig. 3c).

The biantennary, di-sialylated structure (N12, Table 1) varies in abundance over lactation with levels rising between the incompetent and transitional immune stages, then decreasing at the beginning of the competent immune stage, followed by an additional decrease in some individuals around 168 days post-partum (Fig. 3d). The biosynthetic precursors to this glycan (N3 and N10) did not exhibit any detectable consistent temporal trends across individuals ($p>0.05$).

Fig. 3 Box plots show the range of $\log_e$ transformed percentage abundance values plotted over lactation time points. The structures shown in this figure were the only ones found under the linear mixed-effects analysis to have significant temporal changes between at least two time points across all individuals ($p<0.05$). The structures are grouped according to their structural type and listed from left to right in order of their biosynthetic precursors ▶

The *O*-glycome of wallaby milk glycoproteins

Structural analysis of the protein bound *O*-linked oligosaccharides on wallaby milk glycoproteins (*O*-glycome) resulted in the detection of 16 *O*-glycan structures. The majority of the

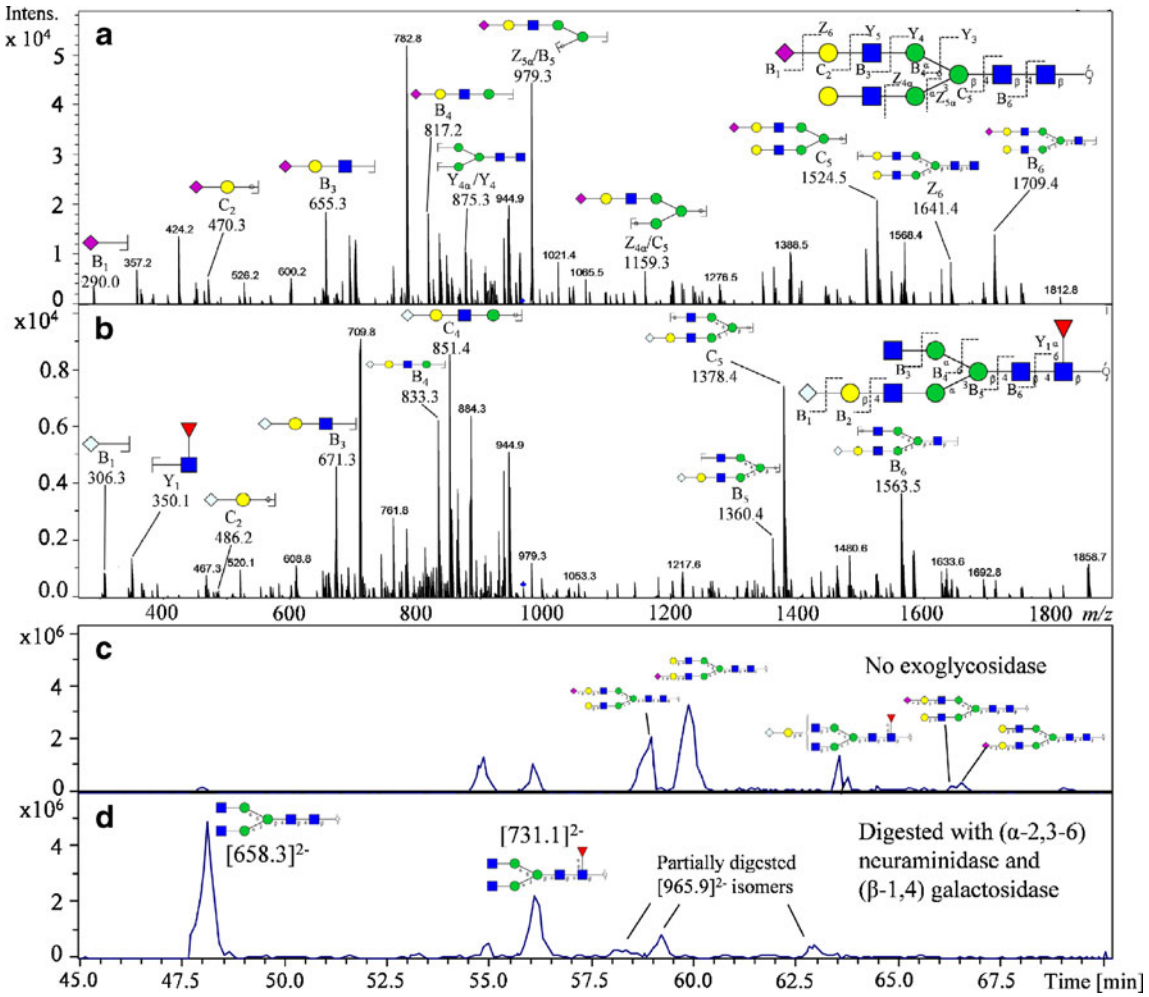

Fig. 2 Investigation of the MS/MS fragmentation of five different LC-MS peaks corresponding to *m/z* $[965.9]^{2-}$ indicated that four peaks correspond to a biantennary *N*-glycan with one *N*-acetylneuraminic acid. A representative MS/MS spectra from the first peak is shown in **a**. The third peak however corresponds to a biantenary core fucosylated *N*-glycan with one *N*-glycolylneuraminic acid (**b**). This was confirmed by digestion with (α-2,3–6) neuraminidase and (β-1,4) galactosidase which resulted in the loss of both the neuraminic acid and galactose moieties on all *m/z* $[965.9]^{2-}$ isomers, with the subsequent signal increase of the resultant structural products, *m/z* $[731.1]^{2-}$ and $[658.3]^{2-}$ (**c & d**). *N*-acetylneuraminic acid containing *m/z* $[965.9]^{2-}$ isomers were differentiated from one another using the *m/z* 979.3 fragment ion for 6′ arm linked *N*-acetylneuraminic acid residues and elution profile from Nakano *et al.* [24]

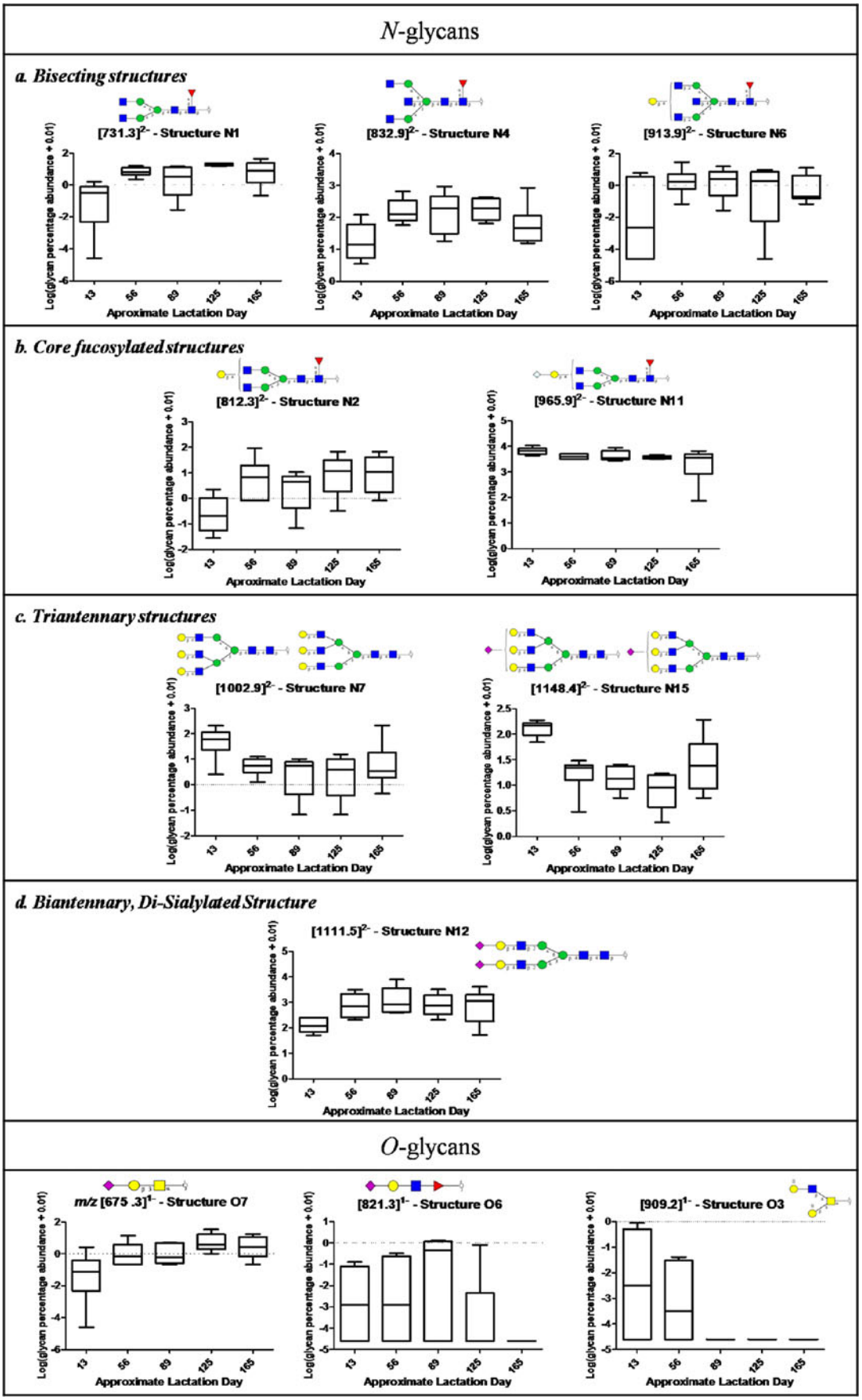
N-glycans
a. Bisecting structures
[731.3]2- - Structure N1
[832.9]2- - Structure N4
[913.9]2- - Structure N6
Log(glycan percentage abundance + 0.01)
Aproximate Lactation Day
Approximate Lactation Day
b. Core fucosylated structures
[812.3]2- - Structure N2
[965.9]2- - Structure N11
c. Triantennary structures
[1002.9]2- - Structure N7
[1148.4]2- - Structure N15
d. Biantennary, Di-Sialylated Structure
[1111.5]2- - Structure N12
O-glycans
m/z [675 .3]1- - Structure O7
[821.3]1- - Structure O6
[909.2]1- - Structure O3
13
56
89
125
165

Table 1 Structures of the most abundant 16*N*-glycan masses (N1-N16) in wallaby milk as confirmed by MS/MS. Where structural isomers and linkages could not be confirmed, only the composition is presented. 11 low abundance *N*-glycan masses (n1-n11) which could not consistently be identified and integrated across samples are also presented but were not used in the linear mixed-effects analysis. Different isomers bring the total number of *N*-linked structures identified to 37. Isomers are listed in order of elution

Mass number	*m/z*	Structure	Mass number	*m/z*	Structure
***N*-glycans**					
Neutral Structures					
N1 [a,b]	$[731.3]^{2-}$		N5 [b]	$[893.4]^{2-}$	
N2 [a,b]	$[812.3]^{2-}$		N6 [a,b]	$[913.9]^{2-}$	
N3	$[820.3]^{2-}$				
N4 [a,b]	$[832.9]^{2-}$		N7 [a]	$[1002.9]^{2-}$	
Sialylated Structures					
N8	$[783.3]^{2-}$		N12 [a]	$[1111.5]^{2-}$	
N9	$[892.2]^{2-}$			$[1111.5]^{2-}$	
N10	$[965.9]^{2-}$		N13 [b]	$[1046.9]^{2-}$	
	$[965.9]^{2-}$		N14 [b]	$[1067.4]^{2-}$	
	$[965.9]^{2-}$		N15 [a]	$[1148.4]^{2-}$	
	$[965.9]^{2-}$			$[1148.4]^{2}$	
N11 [a,b]	$[965.9]^{2-}$			$[1148.4]^{2}$	
			N16	$[1294.0]^{2-}$	
Low Abundance Neutral Structures:			Low Abundance Sialylated Structures:		
n1	$[698.3]^{2-}$		n7	$[864.3]^{2-}$	
n2	$[739.3]^{2-}$		n8	$[872.3]^{2-}$	
n3	$[779.3]^{2-}$		n9	$[884.8]^{2-}$	
n4	$[860.3]^{2-}$		n10 [b]	$[1038.9]^{2-}$	
n5	$[941.4]^{2-}$				
n6	$[1022.4]^{2-}$		n11	$[1119.4]^{2-}$	

Fucose, Mannose, *N*-acetylglucosamine, *N*-glycolyl neuraminic acid, Galactose, *N*-acetylgalactosamine, *N*-acetyl neuraminic acid, Sulphate

[a] Structures exhibiting temporal changes consistently (linear mixed effects p-value<0.05) over lactation across six individual wallabies. These trends are depicted in box plots in Fig. 3

[b] Core fucosylated structures

structures identified were of the *O*-GalNAc linked mucin-type core 2 (68.7 %) (O1- 4, O9, O11-14, Table 2) with and without NeuAc. In a marked difference to the *N*-glycome, no NeuGc containing structures were identified. 18.7 % of structures were of *O*-GalNAc linked mucin-type core 1 (O7, O8 and O10, Table 2).

Table 2 Structures of the 14 *O*-glycan masses in wallaby milk as confirmed by MS/MS. Different isomers bring the total number of *O*-linked structures identified to 16. Where structural isomers and linkages could not be confirmed, only the composition is presented

Mass number	*m/z*	Structure	Mass number	*m/z*	Structure
***O*-glycans**					
Sulphated Structures			***Sialylated Structures***		
O1	$[829.2]^{1-}$		O7 [a]	$[675.3]^{1-}$	
			O8	$[675.3]^{1-}$	
O2	$[829.2]^{1-}$		O9	$[878.4]^{1-}$	
O3 [a]	$[909.2]^{1-}$		O10	$[966.4]^{1-}$	
			O11	$[1040.4]^{1-}$	
O4	$[1120.4]^{1-}$	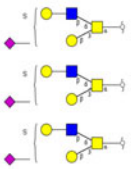	O12	$[1331.5]^{1-}$	
***O*-fucosylated Structures**			***Neutral Structures***		
O5	$[530.3]^{1-}$	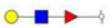	O13	$[587.3]^{1-}$	
O6 [a]	$[821.3]^{1-}$		O14	$[749.3]^{1-}$	
		Fucose; Galactose; *N*-acetylglucosamine; *N*-acetylgalactosamine; *N*-acetyl neuraminic acid; S Sulphate			

[a] Structures exhibiting temporal changes consistently (linear mixed effects p-value<0.05) over lactation across six individual wallabies. These trends are depicted in box plots in Fig. 3

Interestingly, 12.5 % of the *O*-linked structures were the unusual *O*-fucose linked tri- and tetrasaccharides of the composition NeuAcHexHexNAcFuc (O6, Table 2) and HexHexNAcFuc (O5, Table 2). The nature of the direct *O*-fucose linkage to the amino acid backbone was unambiguously identified by MS/MS detection of the ions of *m/z* 165.1 and 350.1 Da, that are diagnostic of fucose at the reducing end of the released oligosaccharide, and which is in accordance with the spectra of presented by Wilson *et al.* (as shown in reference 46, Figure 8).

Another group of potential functionally-interesting *O*-linked glycans were identified by this study. Compositional analysis of *m/z* $[909.2]^{1-}$, $[1120.4]^{1-}$ and two isoforms of *m/z* $[829.3]^{1-}$ (Table 2: O3, O4, O1 and O2, respectively), indicated the presence of a 80 Da sulphate or phosphate group on these structures. To determine whether this was a sulphate residue loss, released *O*-glycans were digested with phosphatase in a separate experiment. Phosphatase activity was confirmed using a glycan sample from *Trichoderma reesii* known to contain Man-PO_4 phosphorylated *N*-glycans [26], while no mass shift was observed for the phosphatase treated wallaby *O*-glycans, indicating that the *O*-glycans were sulphated and not phosphorylated. Also, phosphorylated glycans predominantly have the phosphate addition on a mannose residue and so far no phosphorylated *O*-glycans have been reported in the literature. Sulphate residues were therefore assigned in structures O1 - O4 to the galactose residues of the core 2-type *O*-glycans due to the presence of the B1 *m/z* 241.0 diagnostic fragment ion [27] seen in all four structures (see Fig. 4 for a representative MS/MS of the *m/z* $[829.3]^{1-}$ isoforms). Although the presence of low intensity *m/z* 284 (Panel a, Fig. 4) and 301 (Panel b, Fig. 4) ions indicates sulphation of the *N*-acetylglucosamine moiety and not the outer arm galactose residues, these fragments are most likely present due to sulphate migration from the galactose residue during CID as recently described by Kenny *et al.* [27].

Statistical analysis of temporal changes of the O-glycome

As was seen for the *N*-glycans, the *O*-glycan BPCs indicated that global temporal changes in milk protein *O*-glycosylation occurred across the lactation time in all individuals (Figure 4, Supp data). Only minimal inter-animal variations were seen by qualitative comparison of the average MS spectra of the six different wallaby individuals at each time point (Figure 3, Supp data), however, box plot visualization of the percentage abundance values for those structures were found to be different under the linear mixed effects analysis and demonstrated a high degree of inter-animal variation of each structure. Although there were fewer *O*-glycan structures identified than *N*-glycans, the overall *O*-glycan BPC signal intensities were higher which allowed all structures to be annotated and integrated across samples. Because of this,

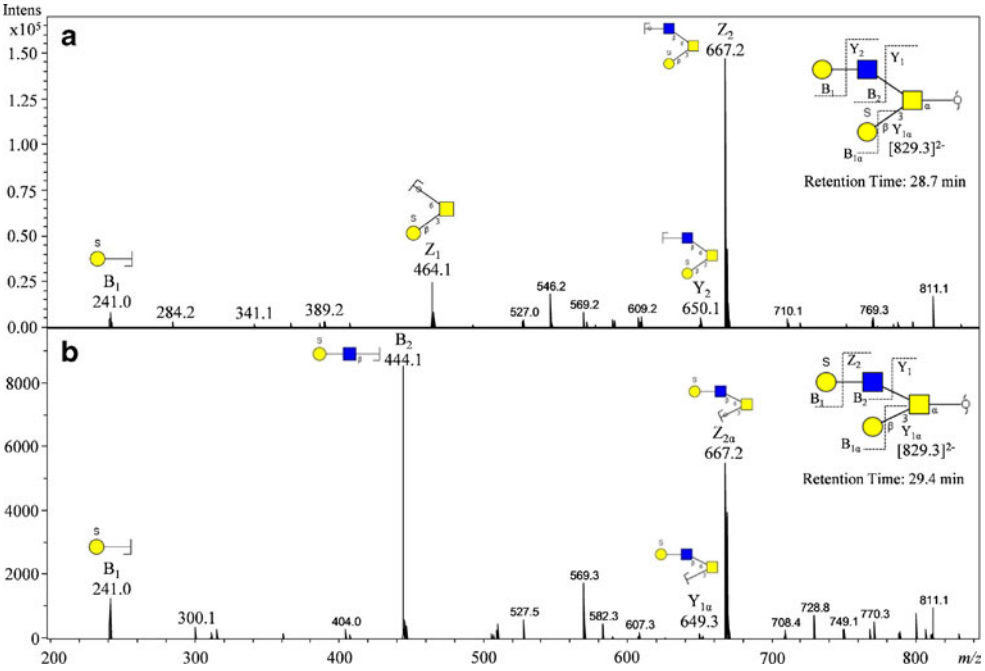

Fig. 4 MS/MS spectra were annotated for the elucidation of the *m/z* $[829.3]^{1-}$ compositional isomers at 28.7 min (**a**) and 29.4 min (**b**). Sulphate residues were assigned to the galactose residues of these structures due to the presence of the B_1 *m/z* 241.0 diagnostic fragment ion [51]. The presence of low intensity *m/z* 284 (**a**) and *m/z* 301 (**b**) ions indicates sulphation of the *N*-acetylglucosamine moiety, however these fragments are most likely present due to sulphate migration from the galactose residue during CID as recently described by Kenny *et al.* [51]

all *O*-glycan structures were included for statistical analysis and none classified as 'low abundance' (as were Structures n1-11 (Table 1) in the *N*-glycome). Three structures, *m/z* $[675.3]^{1-}$, $[821.3]^{1-}$, and $[909.2]^{1-}$ had $p<0.05$ under the mixed-effects analysis and their temporal trends over the lactation sample time points are shown in Fig. 3 (Table 2: O7, O6 and O3 respectively).

PGC-LC ESI-MS/MS analysis allowed separation of two structural isomers of *m/z* $[675.3]^{1-}$ (O7 and O8, Table 2) (Fig. 5a & b). Interestingly, the linear mixed effects model showed only O7 to significantly change in average abundance levels over the lactation period, with an increase during the transitional immune system development stage before decreasing as the immune system reaches competency whereas its isomer, O8 did not (Fig. 5c).

Whilst the non-sialylated *O*-fucosylated structure (O5) was found in all six individuals, its sialylated counterpart (O6, Table 2) was only detected in three of the six individuals analysed. Nevertheless the linear mixed effects model showed a statistically significant abundance change only in the latter. In the three individuals there was a clear increase from the beginning of lactation through to approximately 88 days, where expression then disappeared altogether (bottom panel, Fig. 3). Interestingly, at this stage the immune system of the young is now competent.

The statistical analysis of the sulphated *O*-linked structures showed that only the doubly sulphated *m/z* $[909.2]^{1-}$ (O3) exhibited consistent temporal changes between individuals over lactation. Although this structure was expressed in only three individuals, a marked decrease in abundance was observed over the first two time points with no expression seen in the last three time points (bottom panel, Fig. 3).

Discussion

Approximately 30 % of the *N*-glycans identified on tammar wallaby milk glycoproteins contained core (α1-6) fucosylated structures with no antenna fucosylation identified. (α1,6) fucosyltransferase catalyses the attachment of a fucose moiety to the innermost *N*-acetylglucosamine residue of an *N*-linked glycan core of mammalian glycans, causing a structural change and potentially changing the role and function of the glycoprotein [28]. Core fucosylation in placental mammals is crucial in the binding of epidermal growth factor receptor to its ligand, which subsequently stimulates cell differentiation and growth [29]. Studies of (α1,6) fucosyltransferase double knockout mice lacking this enzyme have observed growth retardation and early death during post-natal development [30] due to disruption of tyrosine kinase activity in the EGFR stimulated cell-signalling pathway [29]. Thus it is possible that core fucosylated glycans on wallaby milk glycoproteins may also be involved supporting the development of the wallaby young. In addition, predominantly core fucosylated glycans of human milk lactoferrin have been reported to be involved in the prevention of bacterial binding to gut epithelial cells and infection [31]. Of the 11 core fucosylated *N*-linked oligosaccharide structures identified here in wallaby milk, five structures exhibited similar temporal trends across lactation in six different individuals. While the direction of the trends is not all the same for the five structures, this may be due to their involvement in different specific processes at different stages of lactation. Overall, the degree of *N*-glycan fucosylation in wallaby milk glycoproteins (30 %) is

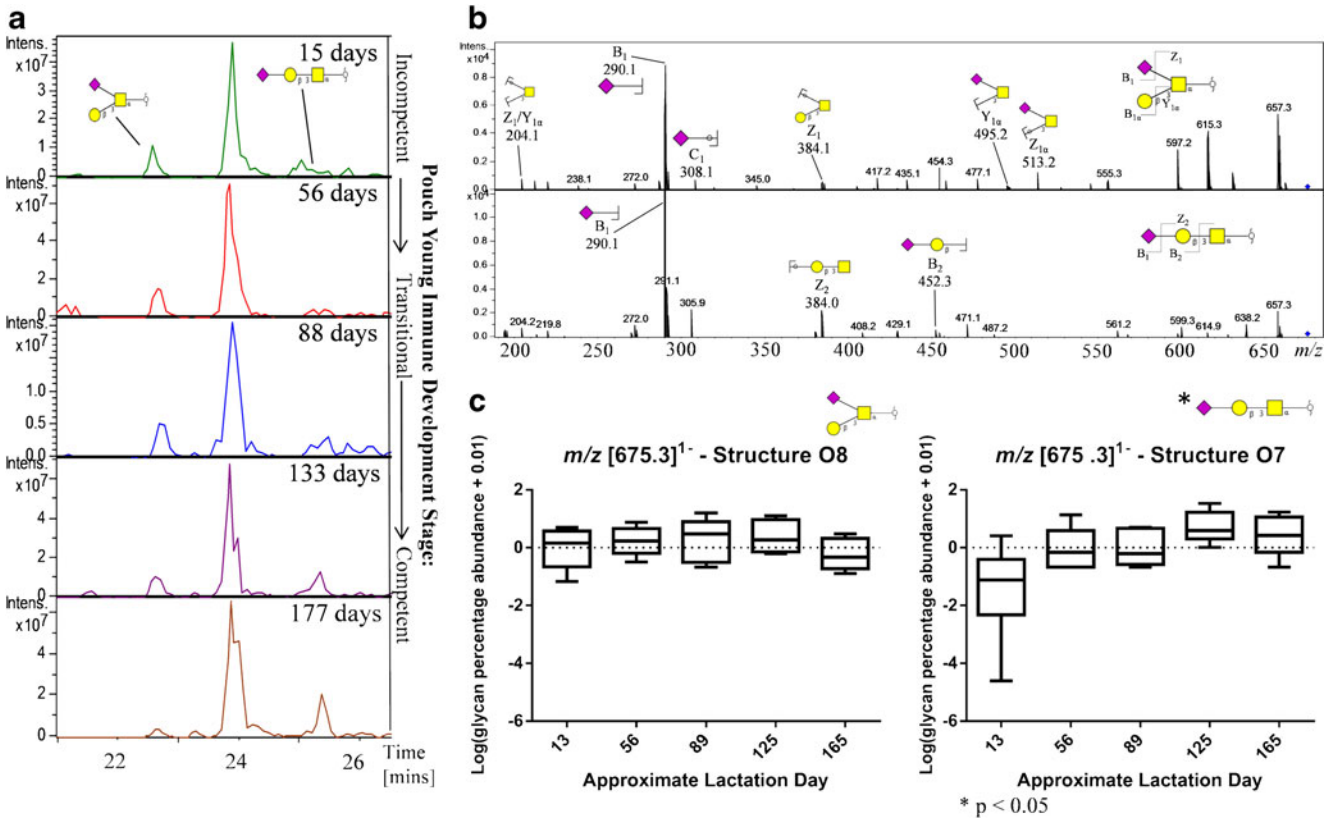

Fig. 5 **a** BPCs between 21 and 27 min showing the lactation time course of the *O*-glycans released from the glycoproteins of one wallaby mother. All time points from 15 to 77 days lactation have been normalized to the major peak in the sample and the $[675.3]^{1-}$ isomer peaks separated by porous graphitized carbon liquid chromatography can be seen on either side. **b** Subsequent MS/MS fragment spectra of the two peaks allowed the different structural isomers to be characterized. MS/MS spectra of the linear $[675.3]^{1-}$ structure showed a prominent loss of an *N*-acetylneuraminic acid therefore the spectra scale was magnified to visualize the low abundance peaks. **c** Box plots depicting the $\log_e$ transformed percentage abundance of the two compositional isomers in all six individuals over lactation time indicate that the temporal trends are not the same for both structures. Only the linear isomer (O7) exhibited a statistically significant trend under the linear mixed-effects analysis ($p<0.05$) with an increase over time across all individuals

less than that reported in human milk (75 %), but similar to bovine milk (31 %) [32].

Core fucosylation is also a modification characteristic of Immunoglobulin G (IgG) glycosylation [33]. IgG has been well documented in the milk of several mammals, including the wallaby, and elicits its immune protective effects by transport across the gut wall into the circulatory system of the young [34, 35]. IgG is present at high levels in wallaby colostrum and milk during the first one hundred days postpartum [36–38] with a subsequent decrease as the pouch young's ability to elicit its own immune response develops. With exception to the NeuGc-containing structures N11, N13 and N14 (see Table 1), all the core fucosylated structures characterised in this study have been previously reported on human serum IgG [39]. IgG glycosylation may therefore be partially contributing to the core fucosylation profile seen in the *N*-glycans of wallaby milk.

Of all the core fucosylated *N*-glycans characterised in wallaby milk, three structures (N4, N6 and N14, Table 1) contain a bisecting GlcNAc attached in (β1-4) linkage to the innermost mannose residue of the *N*-linked glycan core. This feature is known to terminate further *N*-glycan processing and elongation [28] resulting in intermediate *N*-glycan structures (*e.g.* N4, Table 1). Structures similar to N4, N6 and N14 have been reported in early development stages of birds in chicken embryo serum [40], chicken serum IgG [41], and attached to IgY (avian IgG) transferred from serum to egg-yolk in Japanese Quail [42].

Several sialylated *N*-linked glycan structures were found in high abundance (N8-N16, Table 1). These structures may be involved in growth and immune support for the wallaby young since the role of sialic acid containing milk oligosaccharides in inhibiting the binding of pathogens has been documented in humans, such as inhibition of enteropathogenic *Escherichia coli* [2]. Inhibition of rotavirus is thought to be mediated by the sialylated glycans of the lactadherin glycoprotein in human milk, as the protein's ability to inhibit the virus is severely diminished after sialic acid removal [9].

The use of PGC-LC ESI-MS/MS was crucial for unambiguous identification of NeuGc containing core fucosylated glycans (N11, N13 and N14, Table 1). *N*-glycolylneuraminic acid is a commonly found sialic acid in all mammals except humans, new world monkeys and guinea pigs [43] although the sialyltransferase responsible for its addition to glycans is always present [44]. NeuGc acid was identified on six wallaby *N*-linked structures while no *O*-linked glycans were identified carrying this monosaccharide. The overall degree of *N*-glycan sialylation in the tammar wallaby milk (59.6 %) was similar to that of bovine and human milk (68 % and 57 % respectively) [32]. However, taking into consideration that *N*-glycolylneuraminic acid is not expressed in humans, this brings the percentage of structures containing *N*-acetylneuraminic acid residues in wallaby milk (46 %) to below that in human milk.

Mucin type *O*-linked glycans are usually attached to serine or threonine residues *via* an *N*-acetylgalactosamine residue. However, other and rarer types of glycosylation such as the attachment of an *O*-fucosylated oligosaccharide to a serine or threonine have been identified [45]. The MS-MS fragmentation data of the *O*-linked fucose trisaccharide $Hex_1HexNAc_1Fucose_1$ (O5, Table 2) is in very good accordance with the spectra recently reported by Wilson *et al.* [46] who identified the same structure in human milk fat globule membranes (MFGM) but not in bovine MFGM. This structure was first found on epidermal growth factor (EGF)-like domains [47] and the *O*-fucosylation site on EGF itself is evolutionarily conserved [48]. The structure is also involved in intracellular signalling transduction such as the binding of Notch ligands and mediates many cell development and differentiation processes [48]. In Drosophila, the enzyme involved in the addition of an *O*-fucose to Notch receptors, *O*-fucosyltransferase 1, also has chaperone activities and promotes the folding of the receptor protein [49]. Though the highly conserved nature and importance of *O*-fucosylation in cell development is indicated, it has been little studied so we can only speculate about the biological significance for the development of the wallaby. Its presence only in the first stages of lactation is possibly in accordance with the need for this modification only in early development. The sialylated version of this *O*-fucosylated glycan, *m/z* $[821.5]^{1-}$ with composition $Hex_1HexNAc_1Fucose_1NeuAc_1$, (O6, Table 2) has been reported in bovine MFGM, but is not present in human MFGM [46]. *m/z* $[821.5]^{1-}$ exhibited a statistically significant temporal change over lactation while its non-sialylated counterpart did not.

Sulphated glycans are known to be involved in bacterial binding as binding epitopes for *H. pylori* [50], as well as in cell signalling and cell adhesion, growth factor presentation, development and leukocyte homing [51]. Four different structures (O1 - O4, Table 2) were identified as having an additional mass residue of 80 Da, corresponding to the addition of a phosphate or sulphate group to the glycan. Conventional ion traps instruments like the one used in this study unfortunately do not provide the resolution and mass accuracy required for discrimination of these two groups by mass alone. In an earlier study that investigated the sulphation and phosphorylation of different regions of the Dioxin receptor (DR) in mammalian cells, the presence of particular diagnostic ions in the MS/MS were found to distinguish between sulphation or phosphorylation on the peptides [52]. Structures O1-O4 were therefore identified as sulphated by the presence of a 80 Da MS/MS diagnostic ion, as opposed to a 98 Da loss which indicates phosphate presence [52]. It is important to note that the work of Dave *et al.* (2009) used positive ion mode MALDI-TOF-MS for their peptide analysis whereas negative ion mode ion trap MS has been used in the present study. Sulphation was subsequently confirmed when no change in peak intensity in accordance with the loss of a phosphate group was observed after treatment with a phosphatase enzyme. Sulphate residues were thus assigned to the galactose residues of structures O1-O4 due to the presence of the *m/z* 241.0 diagnostic ion [27], although some evidence of sulphate migration to the *N*-acetylglucosamine moiety during CID was also seen. Of these four sulphated *O*-linked glycans, only *m/z* $[909.2]^{1-}$ (O3, Table 2) showed statistically significant temporal changes consistent across six individuals.

It should be noted that the *O*-glycan abundance percentages showed more variability, with a high percentage of zero and missing values. In the case of some structures, while clear trends in the majority of individuals are visible in the raw data, the presence of a single outlier or one individual exhibiting a different trend can mean that the population averages are not found to change significantly over time. Log_e transformation of the data was undertaken to magnify low abundance changes, and these were used to plot the change in percentage abundance over lactation time. This potentially may render the changes in high abundance glycans less obvious. Alternatively it is possible that structures that do not change over time may be involved in providing constant development aid and/or protection to the pouch young over the duration of lactation. For example, all but three sialylated *N*-glycans do not exhibit changes over time thereby suggesting that their action may be necessary to the pouch young over the whole course of lactation.

The detailed structural characterisation of the glycosylation of the proteins in the milk of the marsupial tammar wallaby showed structures similar to those with development and immune protection agents in human milk and reproductive environments in other animals. Some of these structures also changed significantly over lactation across all individuals, indicating their developmental and functional significance in the maternal milk protection of the infant.

Materials and methods

Materials

Immobilon-P Polyvinylidene Fluoride (PVDF) membranes and 10 kDa Microcon ultrafilters were purchased from Millipore (MA, USA). N-Glycosidase F (PNGase F) (recombinant cloned from *Flavobacterium meningosepticum* and expressed in *Escherichia coli*) lyophilized in 10 mM sodium phosphate buffer, pH 7.2, was purchased from Roche Diagnostics (Basel, Switzerland). Ammonium acetate (NH_4COOH), sodium borohydride ($NaBH_4$), Polyvinylpyrrolidone (PVP) 40000 and Direct Blue 71 were obtained from Sigma (St. Louis, MO, USA). AG50W-X8 cation-exchange resin (H^+ − form) was purchased from BioRad (Hercules, CA) and μC_{18} ZipTips from Eppendorf (Hamburg, Germany). (α-2,3–6) Neuraminidase was purchased from Northstar Bioproducts (MA, USA) and (ß-1,4) galactosidase from *Aspergillus oryzae* was kindly provided by Prof. Friedrich Altmann, University of Natural Resources and Applied Life Sciences, Vienna. Alkaline phosphatase and 1x dephosphorylation buffer were obtained from Roche (Germany). HPLC-grade water was obtained using a Milli-Q® Synthesis water purification system (Millipore, MA, USA). ACS grade chloroform, methanol, urea (Fluka Biochemica, Germany), acetic acid (LabServ, Victoria, Australia), and ethanol (Fronine, NSW, Australia) were used in this study.

Wallaby milk sample collection

Wallaby milk samples were collected from six different female tammar wallabies at five time points around 13, 56, 88, 123 and 168 days post-partum. From two of the individuals, only four samples were obtained (around 15, 56, 123 and 168, and 16, 61, 90 and 157 days post-partum respectively), providing a total of 28 samples. However, it was ensured for all individuals that at least one of the four or five samples collected were from each of the three immune development stages of the pouch young: incompetent, transitional and competent [6]. Wallabies where only four samples were collected had one sample missing from either the transitional or competent stage. Samples were collected under approved Animal Ethics protocols (AHEC03/04- 12) obtained by Joss *et al.*, [6] where details of milk collection and treatment prior to freezing can be found.

Milk protein precipitation

Frozen wallaby milk samples were thawed to room temperature and proteins subsequently precipitated using chloroform, methanol and water [based on 53]. Briefly, 8 μl methanol was added to 2 μl of milk sample then vortexed and centrifuged for 10 s. Thirty μl of chloroform was subsequently added and the mixture vortexed until the protein pellet was re-suspended, followed by brief centrifugation once again. For phase separation, 6 μl of water was added and the protein pellet re-suspended. The total mixture was then vortexed at 12, 000*g* for 4 min, resulting in the formation of three layers: a top methanol and water layer, middle protein layer, and a bottom chloroform layer. The chloroform layer was discarded for removal of glycolipids and the remaining two layers dried under vacuum. The protein was re-solubilised with 10 μl 8 M urea and 30 min shaking at 50 °C. Re-solubilised proteins were filtered through a 10 kDa Microcon ultrafilter for 25 min at 12 000*g*, followed by twice washing with 50 μl 8 M urea and 10 mins centrifugation. Ultrafilters were then inverted into fresh eppendorf tubes and spun to collect the milk proteins.

N- and *O*-glycan release from milk glycoproteins

Glycans were released from milk glycoproteins according to Wilson *et al.* [54]. Briefly, to confirm linkages within glycan structures, purified *N*-linked oligosaccharides were digested with 1 μl (α2-3,6) neuraminidase with 0.5 μl (ß-1,4) galactosidase in 100 mM NH_4COOH at 37 °C overnight. Exoglycosidase activity was terminated by heating at 99 °C for 3 min before PGC-LC ESI-MS/MS analysis of the released oligosaccharides.

For differentiation between of sulphate or phosphate modification, purified *O*-glycans were treated with 1 μl alkaline phosphatase in 5 μl 1x dephosphorylation buffer and 5 μl water overnight at 37 °C. As a positive standard for phosphatase activity, an *N*-glycan sample from *Trichoderma reesii* known to contain phosphorylated *N*-glycans was used [26].

Carbon nanoLC ESI-MS/MS

N- and *O*-glycan alditols were analyzed by porous graphitized carbon LC MS/MS on a capillary LC MS/MS using an Agilent MSD ion-trap XCT Plus mass spectrometer coupled to an Agilent 1100 capillary LC (Agilent Technologies, CA USA). The samples were first applied to a Hypercarb PGC HPLC column (5 μm Hypercarb, 0.32×100 mm, Thermo Hypersil, Runcorn UK). *N*-linked oligosaccharides were subsequently separated using a linear gradient with 2–16 % (v/v) ACN/10 mM NH_4HCO_3 for 45 min, followed by a gradient of 16–45 % (v/v ACN/10 mM NH_4HCO_3) for 20 min. The column was then washed with 45 % (v/v) ACN/10 mM NH_4HCO_3 at a flow rate of 5 μl/min for 6 min before re-equilibrating in 10 mM NH_4HCO_3. *O*-linked oligosaccharides were separated using a linear gradient with 0–25 % (v/v) ACN/10 mM NH_4HCO_3 for 25 min, followed by 10 min washing with 72 % (v/v) ACN/10 mM NH_4HCO_3 at a flow rate of 5 μl/min. ESI−MS was performed in negative

ion mode with two scan events: full scan with mass range *m*/*z* 100–2200, and dependent MS/MS scan after collision induced fragmentation. Automated peak recognition and tandem MS of the top 3 most intense precursor ions was performed.

The composition of each glycan was determined from the monoisotopic masses of detected ions shown in the base peak (BPC) and extracted ion (EIC) chromatograms, and was verified manually using MS/MS data. Monoisotopic masses were searched using the GlycoMod database (available at http://www.expasy.ch/tools/glycomod) using parameters of±0.6 Daltons to predict the possible glycan compositions corresponding to these masses.

Relative percentage abundance of each glycan structure was calculated by first generating an EIC for each individual glycan mass. Each chromatogram was smoothed using a Gauss algorithm and the peak area/s of each glycan was integrated. This peak area of each glycan was then expressed as a percentage of the total area of the most abundant glycans in the sample. These relative percentage abundances were then used in a statistical linear mixed-effects analysis of the structural differences occurring over the time course of lactation. In the case of *N*-linked glycan samples, the total area of the 16 most abundant masses (N1-N16, Table 1) across all samples was integrated and analysed, and the 14 most abundant *O*-linked masses (O1- O14, Table 2) for *O*-glycan samples. Where a glycan of low abundance was not selected for MS/MS, its peak area was integrated only if 1) the isotopic profile of the glycan mass was present at least twice in succession when scanning through the sample BPC and 2) its retention time matched the retention time of the same mass in another sample where MS/MS had been carried out. Structures n1-n11 (Table 1) could not be consistently identified across samples and were therefore not included in the statistical analysis.

Linear mixed-effects analysis

In order to identify glycans showing different abundance between at least two time points, a linear model with mixed effects [55] was run separately for each glycan, allowing for a fixed time effect and an individual random effect. In the absence of the random effect, the model would be identical to the better known analysis of variance (ANOVA); the mixed model was preferred as it makes allowance for the individual variation observed in the data. The data used consisted of the percentage abundances of the major 16 *N*-glycan and 14 *O*-glycan masses, which were $\log_e$ transformed as the original percentage values were skewed. In samples where particular glycans were not present, a small value (0.01) was added to the zero percentage so that all values could be transformed. Glycans with mixed effect model p-values less than 0.05 were regarded as showing statistically significant temporal changes. All computations were run using the R statistical software programming environment [56], with specific functionality from the *nlme* R package [57]. The R code used is available from the authors upon request.

Temporal trends of structures found to change under the mixed-effects analyses were depicted through box plots to display the range of the data and the degree of inter-individual variability at each time point. Box plots were created using GraphPad Prism version 5.0 for Windows, (GraphPad Software, San Diego California USA, www.graphpad.com)

Acknowledgements The authors thank Lyn Hinds for organizing sample collection, Shingo Miyauchi for his kind donation of *Trichoderma reesii N*-glycan samples and Prof. Friedrich Altmann for providing a ß-1,4 galactosidase enzyme. This research was facilitated by access to the Australian Proteome Analysis Facility established under the Australian Governments National Collaborative Research Infrastructure Scheme.

Conflict of interest The authors have declared no conflict of interest.

References

1. Goldman, A.S.: Evolution of the mammary gland defense system and the ontogeny of the immune system. J Mammary Gland Biol Neoplasia **7**, 277–289 (2002)
2. Newburg, D.S.: Human milk glycoconjugates that inhibit pathogens. Curr. Med. Chem. **6**, 117–127 (1999)
3. Harmsen, H.J.M., Wildeboer-Veloo, A.C.M., Raangs, G.C., Wagendorp, A.A., Klijn, N., Bindels, J.G., Welling, G.W.: Analysis of intestinal flora development in breast-Fed and formula-Fed infants by using molecular identification and detection methods. J. Pediatr. Gastroenterol. Nutr. **30**, 61–67 (2000)
4. Rinne, M., Kalliomaki, M., Arvilommi, H., Salminen, S., Isolauri, E.: Effect of probiotics and breastfeeding on the bifidobacterium and lactobacillus/enterococcus microbiota and humoral immune responses. J. Pediatr. **147**, 186–191 (2005)
5. Oddy, W.H.: Breastfeeding protects against illness and infection in infants and children: a review of the evidence. Breastfeed Rev **9**, 11–18 (2001)
6. Joss, J.L., Molloy, M.P., Hinds, L., Deane, E.: A longitudinal study of the protein components of marsupial milk from birth to weaning in the tammar wallaby (Macropus eugenii). Dev. Comp. Immunol. **33**, 152–161 (2009)
7. Old, J.M., Deane, E.M.: Development of the immune system and immunological protection in marsupial pouch young. Dev. Comp. Immunol. **24**, 445–454 (2000)
8. Capuco, A.V., Akers, R.M.: The origin and evolution of lactation. J. Biol. **8**, 37 (2009)
9. Newburg, D.S., Ruiz-Palacios, G.M., Morrow, A.L.: Human milk glycans protect infants against enteric pathogens. Annu. Rev. Nutr. **25**, 37–58 (2005)
10. Yuan, J.S., Kousis, P.C., Suliman, S., Visan, I., Guidos, C.J.: Functions of notch signaling in the immune system: consensus and controversies. Annu. Rev. Immunol. **28**, 343–365 (2010)
11. Yago, T., Fu, J., McDaniel, J.M., Miner, J.J., McEver, R.P., Xia, L.: Core 1-derived O-glycans are essential E-selectin ligands on neutrophils. Proc. Natl. Acad. Sci. U. S. A. **107**, 9204–9209 (2010)
12. Ohtsubo, K., Marth, J.D.: Glycosylation in cellular mechanisms of health and disease. Cell **126**, 855–867 (2006)

13. Chaturvedi, P., Warren, C.D., Altaye, M., Morrow, A.L., Ruiz-Palacios, G., Pickering, L.K., Newburg, D.S.: Fucosylated human milk oligosaccharides vary between individuals and over the course of lactation. Glycobiology **11**, 365–372 (2001)
14. Marcobal, A., Barboza, M., Froehlich, J.W., Block, D.E., German, J.B., Lebrilla, C.B., Mills, D.A.: Consumption of human milk oligosaccharides by gut-related microbes. J. Agric. Food Chem. **58**, 5334–5340 (2010)
15. Bradbury, J.H., Collins, J.G., Jenkins, G.A., Trifonoff, E., Messer, M.: 13C-N.m.r. Study of the structures of two branched oligosaccharides from marsupial milk. Carbohydr. Res. **122**, 327–331 (1983)
16. Collins, J.G., Bradbury, J.H., Trifonoff, E., Messer, M.: Structures of four new oligosaccharides from marsupial milk, determined mainly by 13C-n.m.r. Spectroscopy. Carbohydr. Res. **92**, 136–140 (1981)
17. Messer, M., Green, B.: Milk carbohydrates of marsupials. II. Quantitative and qualitative changes in milk carbohydrates during lactation in the tammar wallaby (Macropus eugenii). Aust. J. Biol. Sci. **32**, 519–531 (1979)
18. Messer, M., Trifonoff, E.: Structure of a branched tetrasaccharide from marsupial milk. Carbohydr. Res. **102**, 316–320 (1982)
19. Messer, M., Trifonoff, E., Stern, W., Collins, J.G., Bradbury, J.H.: Structure of a marsupial-milk trisaccharide. Carbohydr. Res. **83**, 327–334 (1980)
20. Urashima, T., Saito, T., Tsuji, Y., Taneda, Y., Takasawa, T., Messer, M.: Chemical characterization of sialyl oligosaccharides isolated from tammar wallaby (macropus eugenii) milk. Biochim. Biophys. Acta **1200**, 64–72 (1994)
21. Karlsson, N.G., Schulz, B.L., Packer, N.H., Whitelock, J.M.: Use of graphitised carbon negative ion LC-MS to analyse enzymatically digested glycosaminoglycans. J Chromatogr B Analyt Technol Biomed Life Sci **824**, 139–147 (2005)
22. Pabst, M., Bondili, J.S., Stadlmann, J., Mach, L., Altmann, F.: Mass+retention time=structure: a strategy for the analysis of N-glycans by carbon LC-ESI-MS and its application to fibrin N-glycans. Anal. Chem. **79**, 5051–5057 (2007)
23. Zaia, J.: Mass spectrometry and the emerging field of glycomics. Chem. Biol. **15**, 881–892 (2008)
24. Nakano, M., Saldanha, R., Gobel, A., Kavallaris, M., Packer, N.H.: Identification of glycan structure alterations on cell membrane proteins in desoxyepothilone B resistant leukemia cells. Mol Cell Proteomics **10**, M111.009001 (2011)
25. Harvey, D.J., Royle, L., Radcliffe, C.M., Rudd, P.M., Dwek, R.A.: Structural and quantitative analysis of N-linked glycans by matrix-assisted laser desorption ionization and negative ion nanospray mass spectrometry. Anal. Biochem. **376**, 44–60 (2008)
26. Harrison, M.J., Nouwens, A.S., Jardine, D.R., Zachara, N.E., Gooley, A.A., Nevalainen, H., Packer, N.H.: Modified glycosylation of cellobiohydrolase I from a high cellulase-producing mutant strain of Trichoderma reesei. Eur J Biochem **256**, 119–127 (1998)
27. Kenny, D.T., Issa, S.M.A., Karlsson, N.G.: Sulfate migration in oligosaccharides induced by negative ion mode ion trap collision-induced dissociation. Rapid Commun. Mass Spectrom. **25**, 2611–2618 (2011)
28. Takahashi, M., Kuroki, Y., Ohtsubo, K., Taniguchi, N.: Core fucose and bisecting GlcNAc, the direct modifiers of the N-glycan core: their functions and target proteins. Carbohydr Res 344, 1387–1390 (2009)
29. Wang, X., Gu, J., Ihara, H., Miyoshi, E., Honke, K., Taniguchi, N.: Core fucosylation regulates epidermal growth factor receptor-mediated intracellular signaling. J Biol Chem **281**, 2572–2577 (2006)
30. Wang, X., Inoue, S., Gu, J., Miyoshi, E., Noda, K., Li, W., Mizuno-Horikawa, Y., Nakano, M., Asahi, M., Takahashi, M., Uozumi, N., Ihara, S., Lee, S.H., Ikeda, Y., Yamaguchi, Y., Aze, Y., Tomiyama, Y., Fujii, J., Suzuki, K., Kondo, A., Shapiro, S.D., Lopez-Otin, C., Kuwaki, T., Okabe, M., Honke, K., Taniguchi, N.: Dysregulation of TGF-beta1 receptor activation leads to abnormal lung development and emphysema-like phenotype in core fucose-deficient mice. Proc Natl Acad Sci U S A **102**, 15791–15796 (2005)
31. Barboza, M., Pinzon, J., Wickramasinghe, S., Froehlich, J.W., Moeller, I., Smilowitz, J.T., Ruhaak, L.R., Huang, J., Lonnerdal, B., German, J.B., Medrano, J.F., Weimer, B.C., Lebrilla, C.B.: Glycosylation of human milk lactoferrin exhibits dynamic changes during early lactation enhancing its role in pathogenic bacteria-host interactions. Mol Cell Proteomics **11**, M111.015248 (2012)
32. Nwosu, C.C., Aldredge, D.L., Lee, H., Lerno, L.A., Zivkovic, A.M., German, J.B., Lebrilla, C.B.: Comparison of the human and bovine milk N-glycome via high-performance microfluidic chip liquid chromatography and tandem mass spectrometry. J Proteome Res **11**, 2912–2924 (2012)
33. Huhn, C., Selman, M.H., Ruhaak, L.R., Deelder, A.M., Wuhrer, M.: IgG glycosylation analysis. Proteomics **9**, 882–913 (2009)
34. Yadav, M.: The transmissions of antibodies across the gut of pouch-young marsupials. Immunology **21**, 839–851 (1971)
35. Van de Perre, P.: Transfer of antibody via mother's milk. Vaccine **21**, 3374–3376 (2003)
36. Adamski, F.M., Demmer, J.: Two stages of increased IgA transfer during lactation in the marsupial, trichosurus vulpecula (Brushtail possum). J Immunol **162**, 6009–6015 (1999)
37. Adamski, F.M., Demmer, J.: Immunological protection of the vulnerable marsupial pouch young: two periods of immune transfer during lactation in Trichosurus vulpecula (brushtail possum). Dev Comp Immunol **24**, 491–502 (2000)
38. Daly, K.A., Digby, M., Lefevre, C., Mailer, S., Thomson, P., Nicholas, K., Williamson, P.: Analysis of the expression of immunoglobulins throughout lactation suggests two periods of immune transfer in the tammar wallaby (Macropus eugenii). Vet Immunol Immunopathol **120**, 187–200 (2007)
39. Wada, Y., Azadi, P., Costello, C.E., Dell, A., Dwek, R.A., Geyer, H., Geyer, R., Kakehi, K., Karlsson, N.G., Kato, K., Kawasaki, N., Khoo, K.H., Kim, S., Kondo, A., Lattova, E., Mechref, Y., Miyoshi, E., Nakamura, K., Narimatsu, H., Novotny, M.V., Packer, N.H., Perreault, H., Peter-Katalinic, J., Pohlentz, G., Reinhold, V.N., Rudd, P.M., Suzuki, A., Taniguchi, N.: Comparison of the methods for profiling glycoprotein glycans–HUPO Human Disease Glycomics/Proteome Initiative multi-institutional study. Glycobiology **17**, 411–422 (2007)
40. Jacquinot, P.M., Leger, D., Wieruszeski, J.M., Coddeville, B., Montreuil, J., Spik, G.: Change in glycosylation of chicken transferrin glycans biosynthesized during embryogenesis and primary culture of embryo hepatocytes. Glycobiology **4**, 617–624 (1994)
41. Suzuki, N., Lee, Y.C.: Site-specific N-glycosylation of chicken serum IgG. Glycobiology **14**, 275–292 (2004)
42. Matsuura, F., Ohta, M., Murakami, K., Matsuki, Y.: Structures of asparagine linked oligosaccharides of immunoglobulins (IgY) isolated from egg-yolk of Japanese quail. Glycoconj J **10**, 202–213 (1993)
43. Sanchez-Juanes, F., Alonso, J.M., Zancada, L., Hueso, P.: Glycosphingolipids from bovine milk and milk fat globule membranes: a comparative study. Adhesion to enterotoxigenic Escherichia coli strains. Biol Chem **390**, 31–40 (2009)
44. Varki, A.: Loss of N-glycolylneuraminic acid in humans: Mechanisms, consequences, and implications for hominid evolution. Am J Phys Anthropol **33**, 54–69 (2001)
45. Okajima, T., Matsuura, A., Matsuda, T.: Biological functions of glycosyltransferase genes involved in O-fucose glycan synthesis. J Biochem **144**, 1–6 (2008)
46. Wilson, N.L., Robinson, L.J., Donnet, A., Bovetto, L., Packer, N.H., Karlsson, N.G.: Glycoproteomics of milk: differences in sugar epitopes on human and bovine milk fat globule membranes. J Proteome Res **7**, 3687–3696 (2008)

47. Kentzer, E.J., Buko, A., Menon, G., Sarin, V.K.: Carbohydrate composition and presence of a fucose-protein linkage in recombinant human pro-urokinase. Biochem Biophys Res Commun **171**, 401–406 (1990)
48. Okajima, T., Matsuda, T.: Roles of O-fucosyltransferase 1 and O-linked fucose in notch receptor function. Methods Enzymol **417**, 111–126 (2006)
49. Okajima, T., Xu, A., Lei, L., Irvine, K.D.: Chaperone activity of protein O-fucosyltransferase 1 promotes notch receptor folding. Science **307**, 1599–1603 (2005)
50. Veerman, E.C., Bank, C.M., Namavar, F., Appelmelk, B.J., Bolscher, J.G., Nieuw Amerongen, A.V.: Sulfated glycans on oral mucin as receptors for Helicobacter pylori. Glycobiology **7**, 737–743 (1997)
51. Delcommenne, M., Kannagi, R., Johnson, P.: TNF-alpha increases the carbohydrate sulfation of CD44: induction of 6-sulfo N-acetyl lactosamine on N- and O-linked glycans. Glycobiology **12**, 613–622 (2002)
52. Dave, K.A., Whelan, F., Bindloss, C., Furness, S.G., Chapman-Smith, A., Whitelaw, M.L., Gorman, J.J.: Sulfonation and phosphorylation of regions of the dioxin receptor susceptible to methionine modifications. Mol Cell Proteomics **8**, 706–719 (2009)
53. Wessel, D., Flugge, U.I.: A method for the quantitative recovery of protein in dilute solution in the presence of detergents and lipids. Anal Biochem **138**, 141–143 (1984)
54. Wilson, N.L., Schulz, B.L., Karlsson, N.G., Packer, N.H.: Sequential analysis of N- and O-linked glycosylation of 2D-PAGE separated glycoproteins. J Proteome Res **1**, 521–529 (2002)
55. Pinheiro, J., Bates, D.: Mixed-Effects Models in S and S-PLUS. Springer, New York (2000)
56. R Development Core Team: R: A language and environment for statistical computing. URL http://www.R-project.org/ (2010)
57. Pinheiro, J., Bates, D., DebRoy, S., Sarkar, D., R Development Core Team: *nlme*: Linear and Nonlinear Mixed Effects Models. In. (2010)